Title
Structure of sugar-bound LacY

Journal
Proceedings of the National Academy of Sciences of the United States of America, 111(5)

ISSN
0027-8424

Authors
Kumar, Hemant
Kasho, Vladimir
Smirnova, Irina
et al.

Publication Date
2014-02-04

DOI
10.1073/pnas.1324141111

Peer reviewed

Structure of sugar-bound LacY

Hemant Kumar[a], Vladimir Kasho[b], Irina Smirnova[b], Janet S. Finer-Moore[a], H. Ronald Kaback[b,c,d,1], and Robert M. Stroud[a,1]

[a]Department of Biochemistry and Biophysics, University of California, San Francisco, CA 94158; and [b]Departments of Physiology, [c]Microbiology, Immunology and Molecular Genetics, and [d]Molecular Biology Institute, University of California, Los Angeles, CA 90095

Contributed by H. Ronald Kaback, December 30, 2013 (sent for review December 21, 2013)

Here we describe the X-ray crystal structure of a double-Trp mutant (Gly46→Trp/Gly262→Trp) of the lactose permease of *Escherichia coli* (LacY) with a bound, high-affinity lactose analog. Although thought to be arrested in an open-outward conformation, the structure is almost occluded and is partially open to the periplasmic side; the cytoplasmic side is tightly sealed. Surprisingly, the opening on the periplasmic side is sufficiently narrow that sugar cannot get in or out of the binding site. Clearly defined density for a bound sugar is observed at the apex of the almost occluded cavity in the middle of the protein, and the side chains shown to ligate the galactopyranoside strongly confirm more than two decades of biochemical and spectroscopic findings. Comparison of the current structure with a previous structure of LacY with a covalently bound inactivator suggests that the galactopyranoside must be fully ligated to induce an occluded conformation. We conclude that protonated LacY binds D-galactopyranosides specifically, inducing an occluded state that can open to either side of the membrane.

X-ray structure | membrane protein | transport | conformational change | induced fit

The lactose permease of *Escherichia coli* (LacY), a paradigm for the major facilitator superfamily (MFS), binds and catalyzes transport of D-galactose and D-galactopyranosides specifically with an H^+ (1, 2). In contrast, LacY does not recognize D-glucose or D-glucopyranosides, which differ only in the orientation of the C4-OH of the pyranosyl ring. By using the free energy released from the energetically downhill movement of H^+ in response to the electrochemical H^+ gradient ($\Delta\tilde{\mu}_{H^+}$), LacY catalyzes the uphill (active) transport of galactosides against a concentration gradient. Because coupling between sugar and H^+ translocation is obligatory, in the absence of $\Delta\tilde{\mu}_{H^+}$, LacY also can transduce the energy released from the downhill transport of sugar to drive uphill H^+ transport with the generation of $\Delta\tilde{\mu}_{H^+}$, the polarity of which depends upon the direction of the sugar gradient.

It also has been shown that LacY binds sugar with a pK_a of ~10.5 and that sugar binding does not induce a change in ambient pH; both findings indicate that the protein is protonated over the physiological range of pH (3–5). These observations and many others (1, 2) provide evidence for an ordered kinetic mechanism in which protonation precedes galactoside binding on one side of the membrane and follows sugar dissociation on the other side. Recent considerations (6) suggest that a similar ordered mechanism may be common to other members of the MFS.

Because equilibrium exchange and counterflow are unaffected by imposition of $\Delta\tilde{\mu}_{H^+}$, it is apparent that the alternating accessibility of sugar- and H^+-binding sites to either side of the membrane is the result of sugar binding and dissociation and not of $\Delta\tilde{\mu}_{H^+}$ (reviewed in refs. 1 and 2). Moreover, downhill lactose/H^+ symport from a high to a low lactose concentration exhibits a primary deuterium isotope effect that is not observed for $\Delta\tilde{\mu}_{H^+}$-driven lactose/H^+ symport, equilibrium exchange, or counterflow (7, 8). Thus, it is likely that the rate-limiting step for downhill symport is deprotonation (9, 10), whereas in the presence of $\Delta\tilde{\mu}_{H^+}$ either dissociation of sugar or a conformational change leading to deprotonation is rate-limiting.

X-ray crystal structures of WT LacY (11), the conformationally restricted mutant C154G (12, 13), and a single-Cys mutant with covalently bound methanethiosulfonyl-galactopyranoside (MTS-Gal) (14) have been determined in an inward-facing conformation. The structures consist of two six-helix bundles that are related by a quasi twofold symmetry axis in the membrane plane, linked by a long cytoplasmic loop between helices VI and VII. Furthermore, in each six-helix bundle, there are two three-helix bundles with inverted symmetry (6, 15). The two six-helix bundles surround a deep hydrophilic cavity tightly sealed on the periplasmic face and open only to the cytoplasmic side (an inward-open conformation). Although crystal structures reflect only a single lowest-energy conformation under conditions of crystallization, the entire backbone appears to be accessible to water (16–18), and an abundance of biochemical and spectroscopic data (19–27) demonstrate that sugar binding causes the molecule to open alternatively to either side of the membrane, thereby providing strong evidence for an alternating-access model (reviewed in refs. 28 and 29).

The initial X-ray structure of conformationally restricted C154G LacY was obtained with density at the apex of the central cavity, but because of limited resolution, the identity of the bound sugar at this site and/or side-chain interactions are difficult to specify with certainty. However, biochemical and spectroscopic studies show that LacY contains a single galactoside-binding site and that the residues involved in sugar binding are located at or near the apex of the central cavity. Although the specificity of LacY is strongly directed toward the C4-OH of the galactopyranosyl ring, other OH groups also are important in the following order: C4-OH >> C6-OH > C3-OH > C2-OH (30, 31). Cys-scanning mutagenesis, site-directed alkylation, and direct binding assays show that Glu126 (helix IV) and Arg144

Significance

The lactose permease of *Escherichia coli* (LacY), a model for the major facilitator superfamily, catalyzes the symport of a galactopyranoside and an H^+ across the membrane by a mechanism in which the sugar-binding site in the middle of the protein becomes alternately accessible to either side of the membrane. However, all X-ray structures thus far show LacY in an inward-facing conformation with a tightly sealed periplasmic side. Significantly, by using a double-Trp mutant, we now describe an almost occluded, outward-open conformation with bound sugar, confirming more than two decades of biochemical and biophysical findings. We also present evidence that protonated LacY specifically binds D-galactopyranosides, inducing an occluded state that can open to either side of the membrane.

Author contributions: V.K., I.S., and H.R.K. designed research; H.K. and J.S.F.-M. performed research; H.K., V.K., I.S., J.S.F.-M., and R.M.S. analyzed data; and H.K., H.R.K., and R.M.S. wrote the paper.

The authors declare no conflict of interest.

Data deposition: The atomic coordinates and structure factors have been deposited in the Protein Data Bank, www.pdb.org (PDB ID code 4OAA).

[1]To whom correspondence may be addressed. E-mail: rkaback@mednet.ucla.edu or stroud@msg.ucsf.edu.

This article contains supporting information online at www.pnas.org/lookup/suppl/doi:10.1073/pnas.1324141111/-/DCSupplemental.

(helix V) are irreplaceable for substrate binding and probably are charge-paired (4, 32–35). Trp151 (helix V), two turns removed from Arg144, stacks aromatically with the galactopyranosyl ring (36, 37). Glu269 (helix VIII), another irreplaceable residue (38–40), also is essential for sugar recognition and binding and cannot be replaced even with Asp without markedly decreasing affinity (4, 41). It has been shown recently (42) that Asn272 (helix VIII) also is essential for binding and transport. In contrast, Cys148 (helix V), which is protected from alkylation by substrate, and Ala122 (helix IV), where bulky replacements make LacY specific for galactose, are close to the binding site but probably do not contact the sugar directly.

Among the conserved residues in LacY and other MFS members are two Gly–Gly pairs between the N- and C-terminal six-helix bundles on the periplasmic side of LacY at the ends of helices II and XI (Gly46 and Gly370, respectively) and helices V and VIII (Gly159 and Gly262, respectively) (43). When Gly46 (helix II) and Gly262 (helix VIII) are replaced with bulky Trp residues (Fig. 1), transport activity is abrogated with little or no effect on galactoside binding (44). Moreover, site-directed alkylation and stopped-flow binding kinetics indicate that the G46W/G262W mutant is open on the periplasmic side (open outward). In addition, the detergent-solubilized mutant exhibits much greater thermal stability than WT LacY (44).

The G46W/G262W mutant now has been crystallized in the presence of a high-affinity lactose analog. Remarkably, the structure presented here depicts an almost occluded, outward-open conformation with a reliably defined model of the bound sugar molecule.

Results

Global Fold. An X-ray crystal structure of LacY G46W/G262W cocrystallized in the presence of 5 mM β-D-galactopyranosyl-1-thio-β-D-galactopyranoside (TDG) was determined to 3.5-Å resolution (Fig. 1), and, importantly, crystals were not obtained in the absence of an added galactoside. Data collection and refinement statistics are summarized in *SI Appendix*, Table S1. The protein crystallized in a different crystal form and space group than other LacY structures, suggesting an overall tertiary structure different from the previous inward-facing conformations (11–14). Crystals of the G46W/G262W mutant are in space group $C222_1$ with cell dimensions a = 101.6 Å, b = 121.9 Å, and c = 264.0 Å, and the structure was determined by molecular replacement using the partial structure of LacY (13) as the search molecule. The protein occupies 29% of the cell volume.

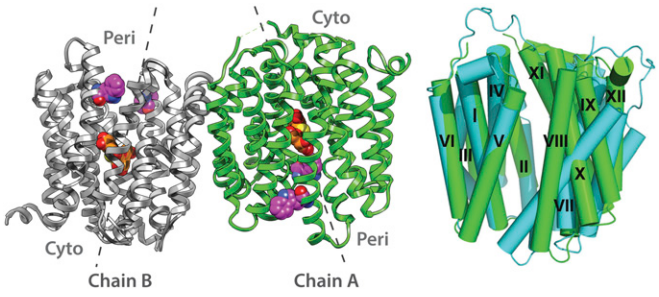

Fig. 1. Side view of LacY G46W/G262W molecules A (*Center*) and B (*Left*) in an almost occluded, outward-facing conformation shown in green and gray ribbons, respectively. The two molecules in the asymmetric unit are shown adjacent to one another from the perspective of the membrane plane. The two molecules have a similar conformation with bound TDG, and the Trp replacements at positions 46 and 262 are shown. TDG and the Trp replacements are represented as spheres, with carbon atoms in magenta (for Trp) or orange (for TDG), oxygen atoms in red, nitrogen atoms in blue, and sulfur in yellow. Dashed lines depict the quasi twofold axes relating the N- and C-terminal helix bundles. (*Right*) The change in structure between LacY G46W/G262W (green; helices numbered) versus the apo WT structure (PDB ID code 2V8N, blue). The orientation matches chain A, and the alignment of the two structures is based on alignment of the N-terminal six-helix bundle of the apo structure onto the G46W/G262W.

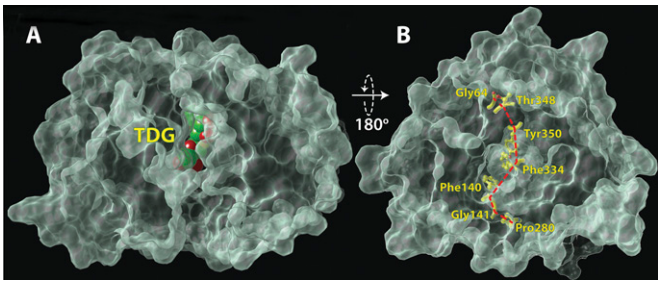

Fig. 2. Surface renditions of LacY G46W/G262W molecule A. (*A*) View from the periplasmic side showing TDG (green and red spheres) just visible within the molecule. (*B*) View from the cytoplasmic side, with the residues that form a zipper-like motif to seal that side portrayed as yellow sticks connected by a broken red line.

Two independent molecules in the asymmetric unit that are adjacent to one another, as if in a bilayer, but have opposite-facing orientations (Fig. 1 and *SI Appendix*, Fig. S1). The Trp replacements on the periplasmic side are illustrated (*SI Appendix*, Fig. S2). Both molecules are in an almost occluded, outward-facing conformation with a single molecule of TDG in the central sugar-binding site. However, the two structures (termed "A" and "B") differ slightly in the substrate orientation and in the arrangement of substrate-binding side chains, suggesting that they sample nearby states around the same part of the transport cycle. A space-filling view of molecule A from the periplasmic side (Fig. 2*A*) reveals bound TDG through an opening that is too narrow to allow entrance or exit (~3 Å at the narrowest point) (45). In contrast, the cytoplasmic side of the molecule is tightly sealed with residues Glu64 (helix II), Thr348 (helix XI), Tyr350 (helix XI), Phe334 (helix X), Phe140 (helix V), Gly141 (helix V), and Pro280 (helix VIII) providing a zipper-like motif (Fig. 2*B*).

The overall rmsd between 380 Cαs of the mutant with bound TDG and WT LacY without any substrate bound [Protein Data Bank (PDB) ID code 2V8N] is 4.3 Å, consistent with very different states. Difference–distance analysis identifies two rigid bodies in these structures, one comprising most of the N-terminal helix bundle (168 residues) and the other comprising most of the C-terminal helix bundle (188 residues); the Cαs can be separately superimposed with rmsds of 1.2 Å. Thus, the mutant structure is related to WT apo LacY by an approximately 30° rotation of one rigid domain against the other about an axis perpendicular to the membrane plane. (Fig. 1 and *SI Appendix*, Fig. S3). Helix VI moves ~12 Å closer to helix VII, and helix IV moves ~12 Å closer to helix IX on the cytoplasmic side. The relative displacements of all helices are listed in *SI Appendix*, Tables S2 and S3.

Substrate-Binding Site. The conformation of the high-affinity TDG molecule is clearly defined in the almost occluded central cavity (Figs. 1 and 3) and allows assignment of likely hydrogen-bond interactions with the protein (*SI Appendix*, Table S4), although the errors in interatomic distances are high at 3.5-Å resolution. Electron density for the sugar is seen in an omit map after refinement without TDG (*SI Appendix*, Fig. S4). The sugar is bound in a manner that is highly consistent with previous mutational, functional, and spectroscopic analyses (reviewed in refs. 1, 2, and 46).

One of the galactopyranosyl rings of TDG lies against Trp151 (helix V), confirming biochemical (36) and spectroscopic (37) findings that indicate hydrophobic stacking between the bottom of the galactopyranosyl ring and the indole ring of the aromatic Trp side chain (Fig. 4). Although Trp151 can be replaced with Tyr or Phe, progressively decreased affinity is observed, and total

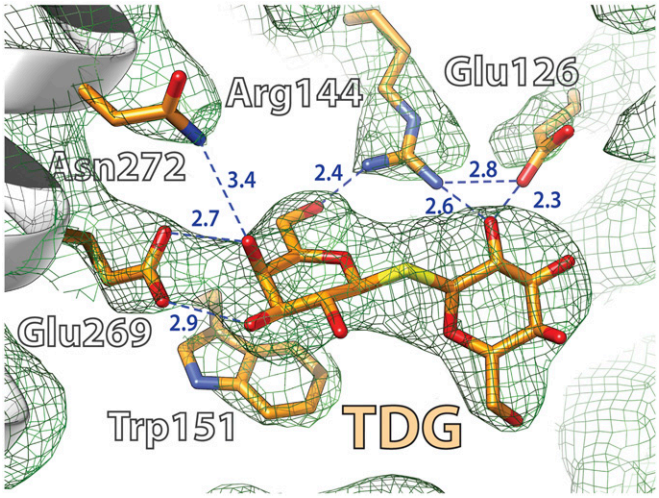

Fig. 3. 2mFo-DFc electron density in a B-factor–sharpened map contoured at 1σ (green mesh) at the sugar-binding site of LacY G46W/G262W, molecule A. The density is superimposed on the structure, which is shown as sticks, with carbon atoms in gold, oxygen atoms in red, and nitrogen atoms in blue. Broken lines represent putative hydrogen bonds.

replacement of the aromatic side chain at position 151 completely abolishes binding and transport. In addition, a red shift in the phosphorescence spectrum of single-Trp151 LacY observed upon sugar binding is explained by their apposition in the structure.

Glu269 (helix VIII) is the acceptor of hydrogen bonds from the C4-OH group of the galactopyranosyl ring, making it a likely candidate for a primary role in specificity. The structure explains the finding that even conservative replacement with an Asp abolishes binding and inactivates transport (4, 39, 47).

The η1 NH_2 group of Arg144 (helix V) donates a hydrogen bond to O5 in the ring and also is within hydrogen-bond distance of C6-OH. The η2 NH_2 group of Arg144 donates hydrogen bonds to C2′-OH of TDG and to Glu126 Oε2 (Fig. 4). Conservative replacement of Arg144 with Lys or neutral replacements virtually destroys binding and transport (4, 32).

Glu126 (helix IV) acts as hydrogen-bond acceptor from the C2′-OH of TDG, explaining why conservative replacement with Asp causes markedly diminished binding affinity and removal of the carboxyl group abolishes binding and transport (4, 33).

His322 (helix X) acts as a hydrogen-bond donor/acceptor between the εNH of the imidazole ring and the C3-OH of TDG and is stabilized by a hydrogen-bond donor/acceptor with the δNH of the imidazole and the OH of Tyr236. All replacements for His322 tested exhibit a marked decrease in binding affinity and little or no transport activity (4, 48, 49).

Finally, Asn272 (helix VIII) likely donates a hydrogen bond to the C4-OH of TDG, confirming the recent biochemical finding (42) indicating that Asn272 also plays an essential role in sugar binding. Gln is the only replacement that is well tolerated by LacY.

Additional Important Residues. In addition to the residues that play a direct role in galactoside binding, Cys148 (helix V), well known with respect to substrate protection against alkylation (reviewed in ref. 46), is close to bound TDG but is not sufficiently close to interact directly. Similarly, replacement of Ala122 (helix IV) with bulky side chains or alkylation of A122C with bulky thiol reagents causes LacY to become specific for the monosaccharide galactose, and disaccharide binding and transport are blocked (50). However, Ala122 does not make direct contact with TDG.

Asp240 (helix VII) and Lys-319 (helix X) are weakly salt bridged (51, 52), and mutation of either residue does not markedly alter affinity (4).

Glu325 (helix X) and Arg302 (helix IX) (Figs. 4 and 6) are directly involved in coupled H^+ translocation. Neutral replacement of either residue yields mutants that are defective in all transport reactions that involve lactose/H^+ symport but catalyze equilibrium exchange and/or counterflow as well as or better than WT (1, 2). Neither residue is sufficiently close to the bound sugar to make direct contact.

Discussion

The G46W/G262W mutant of LacY described here behaves as if it is arrested in an outward-open conformation with diffusion-limited access to the binding site based on biochemical and spectroscopic measurements (44). The X-ray crystal structure has bound substrate and as a result is almost occluded and still is partially open to the periplasmic side. Moreover, the opening is sufficiently narrow so that bound TDG is too bulky to exit from the binding site without concomitant and concerted structure changes, and the cytoplasmic side appears tightly sealed. A simple explanation is that, in the absence of sugar, the periplasmic pathway in the mutant is sufficiently open to allow access of TDG to the binding site. However, when binding occurs and the mutant attempts to transition into an occluded state, it cannot do so completely because the bulky Trp residues at positions 46 and 262 block complete closure. Thus, the mutant is able to bind sugar and can initiate but cannot complete the transition into an occluded state. Therefore, the mutant is completely unable to catalyze transport of any type across the membrane.

Although crystals of G46W/G262W diffract to 3.5 Å, the density observed in the cavity at the middle of the protein clearly defines the conformation of TDG, and no additives were present during crystallization that might give rise to artifactual densities. Furthermore, crystals of the mutant were obtained only in the presence of a galactopyranoside. It also is highly relevant that the amino acid side chains ligating the sugar in the structure are entirely consistent with extensive biochemical/spectroscopic studies. Finally, as shown in Figs. 5*A* and 6, which are from a study by Chaptal et al. (14) and show the structure of single-Cys122 LacY with covalently bound MTS-Gal, the galactosyl moiety of the inactivator exhibits precisely the same position in the binding site, as shown in Figs. 4 and 6. In addition, two important ligands—Trp151 and Glu269—interact with the galactopyranosyl ring precisely as observed with TDG in the double-Trp mutant (Figs. 3, 4, and 6).

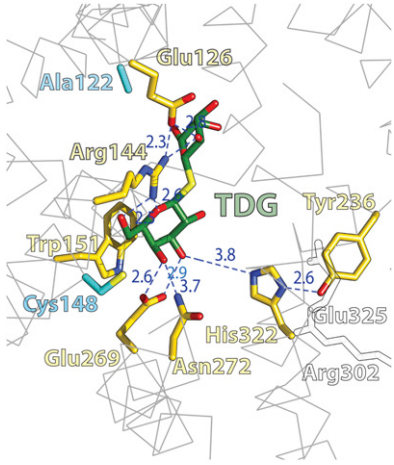

Fig. 4. The sugar-binding site in molecule B. (*A*) TDG is shown as green sticks, and side chains forming hydrogen bonds with TDG are in yellow. Broken lines represent likely hydrogen bonds. Ala122 and Cys148, which are close to TDG but do not make direct contact, are shown in light blue. Glu325 and Arg302 are transparent. For stereo views of the sugar-binding site in both chain A and chain B, see Fig. 6.

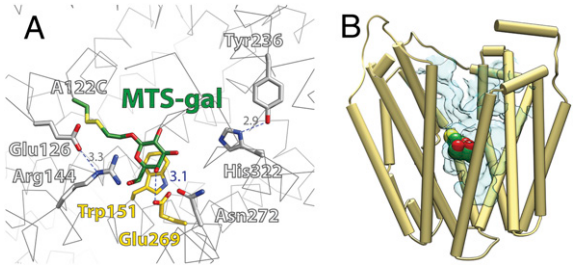

Fig. 5. Crystal structure of single-Cys122 LacY with covalently bound MTS-Gal. (*A*) Helices are displayed as lines for ease of viewing, and side chains are shown as sticks. Side chains in yellow (Glu269 and Trp151) make direct contact with the galactopyranosyl ring of MTS-Gal covalently bound to a Cys at position 122. Side chains in gray are not sufficiently close to make direct contact with the galactopyranosyl ring. For a stereo view of the sugar-binding site, see Fig. 6. (*B*) Structure of single-Cys122 LacY with covalently bound MTS-Gal viewed from the side. Helices are depicted as rods, and MTS-Gal is shown as spheres colored by atom type with carbon ingreen. The water-filled central cavity open on the cytoplasmic side is colored light gray.

Remarkably, as opposed to the almost occluded, open-outward conformation of TDG-bound G46W/G262W, LacY with covalently bound MTS-Gal in the binding site exhibits an inward-open conformation (Fig. 5*B*). This difference clearly suggests that the sugar must be fully ligated to transition into the occluded state. Given this possibility and observations indicating that the alternating access mechanism of LacY is driven by galactoside binding and dissociation, and not by $\Delta\tilde{\mu}_{H^+}$, it seems highly likely that sugar binding involves induced fit. By this means, the N- and C-terminal bundles converge as given side chains from both the N- and C-terminal helix bundles ligate the galactoside. The energetic cost of binding and the resultant conformational change are regained upon sugar dissociation and provide the energy for a further structural change that allows deprotonation. In brief, the mechanism of LacY resembles that of an enzyme, the difference being that the substrate-bound intermediate lies along a structural trajectory from one side to the other.

Another notable implication of the present structure is that Glu269, His322, and Tyr236, long considered by implication to be involved in coupled H^+ translocation (reviewed in refs. 1 and 2), are clearly ligands to the galactopyranoside. Although mutation of these residues causes the periplasmic side of LacY to open spontaneously (53), there is no direct evidence that they are involved in H^+ translocation, although it is conceivable that they may play a dual role in the transport mechanism.

In conclusion, it should be noted that the double-Gly motif observed in LacY that has led to the important and informative structure presented here is conserved in many members of the MFS (43). Thus, the approach of using double- or even tetra-Trp substitutions in the double-Gly motifs may represent a general approach to obtaining structural information about other members of the MFS family, a particularly exciting possibility.

Methods

Materials. TDG was obtained from Carbosynth Limited. Buffers were from Sigma-Aldrich. Talon Superflow Resin was purchased from BD Clontech. Dodecyl-β-D-maltopyranoside (DDM) and n-nonyl-β-D-glucoside (NG) were obtained from Affymetrix. All other materials were of reagent grade and were obtained from commercial sources.

Growth, Expression, and Purification. Plasmid pT7-5 encoding LacY G46W/G262W/His6 was expressed in *E. coli* C41. The detailed procedure is described in *SI Appendix*. Membranes were prepared and solubilized in DDM, and LacY was purified on a Co(II) column and eluted in 20 mM Hepes/0.2% NG/200 mM imidazole (pH 6.5). Details are given in *SI Appendix*.

Crystallization, Data Collection, and Structure Determination. TDG was added (5 mM final concentration) to a protein solution [10 mg/mL in 20 mM Hepes (pH 6.5)/0.2% NG] before crystallization trials. Crystallization screens were set up using the hanging-drop vapor-diffusion method on a Mosquito Crystal Robot (TTP Labtech) in a 96-well plate with a drop ratio of 100 nL well solution:100 nL protein. Crystals appeared in 24 h and grew to 500 × 150 × 150 μm in 1 wk. Crystals were harvested after 7 d and screened for diffraction. Crystals were reproducible and appeared in wide range of PEG concentrations. They also appeared at different pHs and with different buffers. The best-diffracting crystals grew in 1.0 M NaCl/0.05 M Tris (pH 8.0)/24% PEG 600. No cryoprotectant was added before data collection.

Diffraction data were collected at the Lawrence Berkeley National Laboratory Advanced Light Source Beamline 8.3.1, at −170 °C and at a wavelength of 1.115 Å. The highest-resolution crystals diffracted to 3.5 Å. Data were processed with either XDS (54) or HKL2000 (55).

The structure was solved by molecular replacement in PHENIX (56) using LacY 2CFQ as the search model. Coot was used for density fitting (57), and refinement was done with PHENIX (56) and Refmac from the CCP4 suite (58). Hydrogens were included in riding positions. In the final cycles of refinement, translation, libration, screw-motion parameters (59) for a single group (the entire structure) were refined, and Ramachandran angles were restrained. *SI Appendix*, Table S1 shows data and refinement statistics. The MolProbity server (60) was used for structural validation leading to improvement. Difference–distance analysis was done using

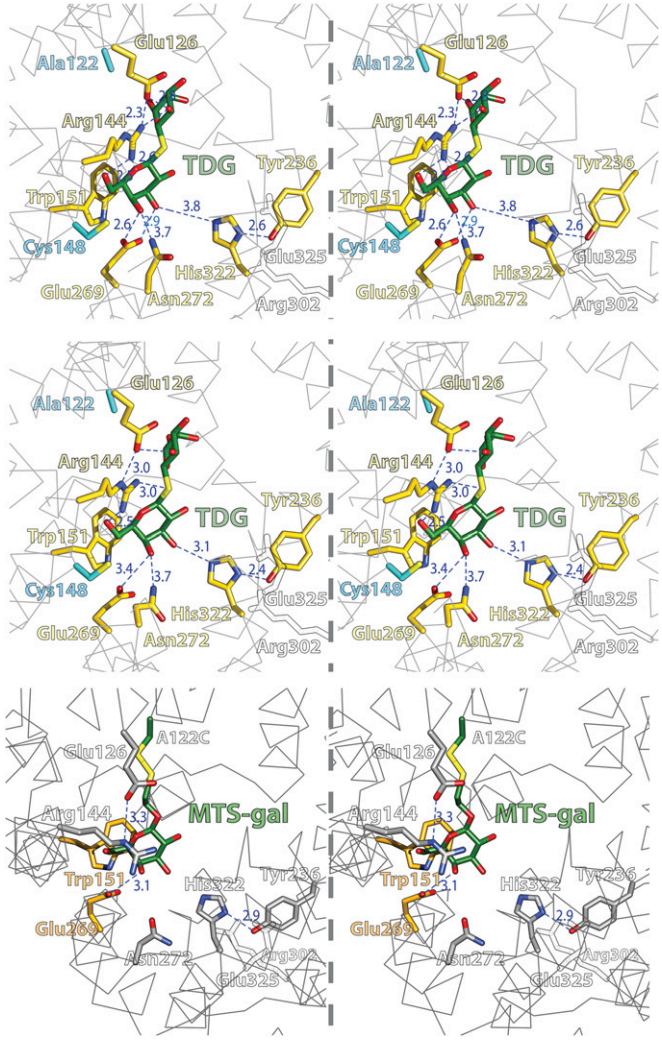

Fig. 6. Stereo view of the sugar-binding site. TDG is shown as green stick model, and side chains forming hydrogen bonds with TDG are in yellow. Ala122 and Cys148, which are close to TDG but do not make direct contact, are shown in cyan. (*Top*) Molecule A with TDG. (*Middle*) Molecule B with TDG. (*Bottom*) LacY with covalently bound MTS-Gal (PDB ID code 2Y5Y).

BIOCHEMISTRY

Rapido (61), and rigid body motions were analyzed using the Dyndom server (62).

ACKNOWLEDGMENTS. We thank M. Gregor Madej for expert help with preparation of many of the figures; Jun-yong Choe, Rosalind Franklin University of Medicine and Science, for data collection at the Advanced Photon Source; Meseret Tessema for cell growth; Joseph D. O'Connell III for help in initial crystal trials; and the Advanced Light Source BM 8.3.1 staff, James Holton, and George Meigs for their help in X-ray data collection. This work was supported by National Institutes of Health Grants DK51131, DK069463, and GM073210, and by National Science Foundation Grants MCB-1129551 (to H.R.K.) and R37GM024485 (to R.M.S.).

1. Guan L, Kaback HR (2006) Lessons from lactose permease. *Annu Rev Biophys Biomol Struct* 35:67–91.
2. Madej MG, Kaback HR (2014) The life and times of Lac permease: Crystals ain't enough. *Membrane Transporter Function: To Structure and Beyond*, eds Ziegler C, Kraemer R (Springer Series in Biophysics: Transporters), in press.
3. Smirnova IN, Kasho V, Kaback HR (2008) Protonation and sugar binding to LacY. *Proc Natl Acad Sci USA* 105(26):8896–8901.
4. Smirnova IN, Kasho VN, Sugihara J, Choe JY, Kaback HR (2009) Residues in the H+ translocation site define the pKa for sugar binding to LacY. *Biochemistry* 48(37): 8852–8860.
5. Smirnova I, Kasho V, Sugihara J, Vázquez-Ibar JL, Kaback HR (2012) Role of protons in sugar binding to LacY. *Proc Natl Acad Sci USA* 109(42):16835–16840.
6. Madej MG, Kaback HR (2013) Evolutionary mix-and-match with MFS transporters II. *Proc Natl Acad Sci USA* 110(50):E4831–E4838.
7. Viitanen P, Garcia ML, Foster DL, Kaczorowski GJ, Kaback HR (1983) Mechanism of lactose translocation in proteoliposomes reconstituted with lac carrier protein purified from *Escherichia coli*. 2. Deuterium solvent isotope effects. *Biochemistry* 22(10): 2531–2536.
8. Gaiko O, Bazzone A, Fendler K, Kaback HR (2013) Electrophysiological Characterization of Uncoupled Mutants of LacY. *Biochemistry* 52(46):8261–8266.
9. Garcia-Celma JJ, Smirnova IN, Kaback HR, Fendler K (2009) Electrophysiological characterization of LacY. *Proc Natl Acad Sci USA* 106(18):7373–7378.
10. Garcia-Celma JJ, Ploch J, Smirnova I, Kaback HR, Fendler K (2010) Delineating electrogenic reactions during lactose/H+ symport. *Biochemistry* 49(29):6115–6121.
11. Guan L, Mirza O, Verner G, Iwata S, Kaback HR (2007) Structural determination of wild-type lactose permease. *Proc Natl Acad Sci USA* 104(39):15294–15298.
12. Abramson J, et al. (2003) Structure and mechanism of the lactose permease of Escherichia coli. *Science* 301(5633):610–615.
13. Mirza O, Guan L, Verner G, Iwata S, Kaback HR (2006) Structural evidence for induced fit and a mechanism for sugar/H+ symport in LacY. *EMBO J* 25(6):1177–1183.
14. Chaptal V, et al. (2011) Crystal structure of lactose permease in complex with an affinity inactivator yields unique insight into sugar recognition. *Proc Natl Acad Sci USA* 108(23):9361–9366.
15. Radestock S, Forrest LR (2011) The alternating-access mechanism of MFS transporters arises from inverted-topology repeats. *J Mol Biol* 407(5):698–715.
16. le Coutre J, Kaback HR, Patel CK, Heginbotham L, Miller C (1998) Fourier transform infrared spectroscopy reveals a rigid alpha-helical assembly for the tetrameric Streptomyces lividans K+ channel. *Proc Natl Acad Sci USA* 95(11):6114–6117.
17. Patzlaff JS, Moeller JA, Barry BA, Brooker RJ (1998) Fourier transform infrared analysis of purified lactose permease: A monodisperse lactose permease preparation is stably folded, alpha-helical, and highly accessible to deuterium exchange. *Biochemistry* 37(44):15363–15375.
18. Sayeed WM, Baenziger JE (2009) Structural characterization of the osmosensor ProP. *Biochim Biophys Acta* 1788(5):1108–1115.
19. Kaback HR, et al. (2007) Site-directed alkylation and the alternating access model for LacY. *Proc Natl Acad Sci USA* 104(2):491–494.
20. Smirnova I, et al. (2007) Sugar binding induces an outward facing conformation of LacY. *Proc Natl Acad Sci USA* 104(42):16504–16509.
21. Majumdar DS, et al. (2007) Single-molecule FRET reveals sugar-induced conformational dynamics in LacY. *Proc Natl Acad Sci USA* 104(31):12640–12645.
22. Zhou Y, Guan L, Freites JA, Kaback HR (2008) Opening and closing of the periplasmic gate in lactose permease. *Proc Natl Acad Sci USA* 105(10):3774–3778.
23. Zhou Y, Nie Y, Kaback HR (2009) Residues gating the periplasmic pathway of LacY. *J Mol Biol* 394(2):219–225.
24. Smirnova I, Kasho V, Sugihara J, Kaback HR (2009) Probing of the rates of alternating access in LacY with Trp fluorescence. *Proc Natl Acad Sci USA* 106(51):21561–21566.
25. Nie Y, Kaback HR (2010) Sugar binding induces the same global conformational change in purified LacY as in the native bacterial membrane. *Proc Natl Acad Sci USA* 107(21):9903–9908.
26. Jiang X, Nie Y, Kaback HR (2011) Site-directed alkylation studies with LacY provide evidence for the alternating access model of transport. *Biochemistry* 50(10):1634–1640.
27. Smirnova I, Kasho V, Sugihara J, Kaback HR (2011) Opening the periplasmic cavity in lactose permease is the limiting step for sugar binding. *Proc Natl Acad Sci USA* 108(37):15147–15151.
28. Kaback HR, Smirnova I, Kasho V, Nie Y, Zhou Y (2011) The alternating access transport mechanism in LacY. *J Membr Biol* 239(1-2):85–93.
29. Smirnova I, Kasho V, Kaback HR (2011) Lactose permease and the alternating access mechanism. *Biochemistry* 50(45):9684–9693.
30. Sahin-Tóth M, Akhoon KM, Runner J, Kaback HR (2000) Ligand recognition by the lactose permease of *Escherichia coli*: Specificity and affinity are defined by distinct structural elements of galactopyranosides. *Biochemistry* 39(17):5097–5103.
31. Sahin-Tóth M, Lawrence MC, Nishio T, Kaback HR (2001) The C-4 hydroxyl group of galactopyranosides is the major determinant for ligand recognition by the lactose permease of *Escherichia coli*. *Biochemistry* 40(43):13015–13019.
32. Frillingos S, Gonzalez A, Kaback HR (1997) Cysteine-scanning mutagenesis of helix IV and the adjoining loops in the lactose permease of Escherichia coli: Glu126 and Arg144 are essential. off. *Biochemistry* 36(47):14284–14290.
33. Sahin-Tóth M, et al. (1999) Characterization of Glu126 and Arg144, two residues that are indispensable for substrate binding in the lactose permease of Escherichia coli. *Biochemistry* 38(2):813–819.
34. Venkatesan P, Kaback HR (1998) The substrate-binding site in the lactose permease of *Escherichia coli*. *Proc Natl Acad Sci USA* 95(17):9802–9807.
35. Wolin CD, Kaback HR (2000) Thiol cross-linking of transmembrane domains IV and V in the lactose permease of Escherichia coli. *Biochemistry* 39(20):6130–6135.
36. Guan L, Hu Y, Kaback HR (2003) Aromatic stacking in the sugar binding site of the lactose permease. *Biochemistry* 42(6):1377–1382.
37. Vázquez-Ibar JL, Guan L, Svrakic M, Kaback HR (2003) Exploiting luminescence spectroscopy to elucidate the interaction between sugar and a tryptophan residue in the lactose permease of *Escherichia coli*. *Proc Natl Acad Sci USA* 100(22):12706–12711.
38. Ujwal ML, Sahin-Tóth M, Persson B, Kaback HR (1994) Role of glutamate-269 in the lactose permease of Escherichia coli. *Mol Membr Biol* 11(1):9–16.
39. Frillingos S, Sahin-Tóth M, Wu J, Kaback HR (1998) Cys-scanning mutagenesis: A novel approach to structure function relationships in polytopic membrane proteins. *FASEB J* 12(13):1281–1299.
40. Weinglass AB, et al. (2003) Elucidation of substrate binding interactions in a membrane transport protein by mass spectrometry. *EMBO J* 22(7):1467–1477.
41. He MM, Kaback HR (1997) Interaction between residues Glu269 (helix VIII) and His322 (helix X) of the lactose permease of Escherichia coli is essential for substrate binding. *Biochemistry* 36(44):13688–13692.
42. Jiang X, Villafierte MKR, Andersson M, White SH, Kaback HR (2013) The galactoside binding site in LacY. *Biochemistry*, in press.
43. Kasho VN, Smirnova IN, Kaback HR (2006) Sequence alignment and homology threading reveals prokaryotic and eukaryotic proteins similar to lactose permease. *J Mol Biol* 358(4):1060–1070.
44. Smirnova I, Kasho V, Sugihara J, Kaback HR (2013) Trp replacements for tightly interacting Gly-Gly pairs in LacY stabilize an outward-facing conformation. *Proc Natl Acad Sci USA* 110(22):8876–8881.
45. Pellegrini-Calace M, Maiwald T, Thornton JM (2009) PoreWalker: A novel tool for the identification and characterization of channels in transmembrane proteins from their three-dimensional structure. *PLOS Comput Biol* 5(7):e1000440.
46. Kaback HR, Sahin-Tóth M, Weinglass AB (2001) The kamikaze approach to membrane transport. *Nat Rev Mol Cell Biol* 2(8):610–620.
47. Sahin-Tóth M, Karlin A, Kaback HR (2000) Unraveling the mechanism of the lactose permease of *Escherichia coli*. *Proc Natl Acad Sci USA* 97(20):10729–10732.
48. Padan E, Sarkar HK, Viitanen PV, Poonian MS, Kaback HR (1985) Site-specific mutagenesis of histidine residues in the *lac* permease of *Escherichia coli*. *Proc Natl Acad Sci USA* 82(20):6765–6768.
49. Püttner IB, Sarkar HK, Poonian MS, Kaback HR (1986) lac permease of Escherichia coli: Histidine-205 and histidine-322 play different roles in lactose/H+ symport. *Biochemistry* 25(16):4483–4485.
50. Guan L, Sahin-Toth M, Kaback HR (2002) Changing the lactose permease of Escherichia coli into a galactose-specific symporter. *Proc Natl Acad Sci USA* 99(10):6613–6618.
51. Sahin-Tóth M, Dunten RL, Gonzalez A, Kaback HR (1992) Functional interactions between putative intramembrane charged residues in the lactose permease of Escherichia coli. *Proc Natl Acad Sci USA* 89(21):10547–10551.
52. Sahin-Tóth M, Kaback HR (1993) Properties of interacting aspartic acid and lysine residues in the lactose permease of Escherichia coli. *Biochemistry* 32(38):10027–10035.
53. Zhou Y, Jiang X, Kaback HR (2012) Role of the irreplaceable residues in the LacY alternating access mechanism. *Proc Natl Acad Sci USA* 109(31):12438–12442.
54. Kabsch W (2010) Xds. *Acta Crystallogr D Biol Crystallogr* 66(Pt 2):125–132.
55. Otwinowski Z, Minor W (1997) Processing of X-ray diffraction data collected in oscillation mode. *Methods Enzymol* 276:307–326.
56. Adams PD, et al. (2010) PHENIX: A comprehensive Python-based system for macromolecular structure solution. *Acta Crystallogr D Biol Crystallogr* 66(Pt 2):213–221.
57. Emsley P, Lohkamp B, Scott WG, Cowtan K (2010) Features and development of Coot. *Acta Crystallogr D Biol Crystallogr* 66(Pt 4):486–501.
58. Winn MD, et al. (2011) Overview of the CCP4 suite and current developments. *Acta Crystallogr D Biol Crystallogr* 67(Pt 4):235–242.
59. Painter J, Merritt EA (2006) Optimal description of a protein structure in terms of multiple groups undergoing TLS motion. *Acta Crystallogr D Biol Crystallogr* 62(Pt 4): 439–450.
60. Chen VB, et al. (2010) MolProbity: All-atom structure validation for macromolecular crystallography. *Acta Crystallogr D Biol Crystallogr* 66(Pt 1):12–21.
61. Mosca R, Schneider TR (2008) RAPIDO: A web server for the alignment of protein structures in the presence of conformational changes. *Nucleic Acids Res* 36(Web Server issue):W42-6.
62. Hayward S, Berendsen HJ (1998) Systematic analysis of domain motions in proteins from conformational change: New results on citrate synthase and T4 lysozyme. *Proteins* 30(2):144–154.

Structure of Sugar-Bound LacY Supplementary information

Methods:

Growth and expression: Plasmid pT7-5 encoding LacY G46W/G262W/His6 was expressed in *E. coli* C41. Transformed cells (colonies from LB/Amp plates) were inoculated into 200 ml of LB/Amp (0.1 mg/ml ampicillin, final concentration) and grown overnight at 37°C on a shaker. 200 ml cultures were inoculated into 10 Litre fermenters, and when the OD_{600} reached 1 (~6hrs after inoculation) 2 mM IPTG was added to induce.

Cells were grown for another 4-5 hrs before harvesting. Cells were harvested and 200 grams of cells were resuspended to 800 ml in 50 mM NaP_i (pH 7.5)/2 mM DTT/25 mg 4-(2-aminoethyl) benzenesulfonyl fluoride hydrochloride (AEBSF)/2 tablets Complete Protease Inhibitor (Sigma Aldrich Corp. USA). A Bead Beater was used to lyse the cells at 0°C using pulses of 1 minute on and 3 minutes off for 10 cycles. Preparations were centrifuged at ~12,000xg for 15 minutes, and the supernatant was centrifuged in Ti45 rotor at 42,000 rpm for 3 h. The membrane pellets were resuspended in 100 ml of 50 mM cold NaP_i (pH 7.5) using a Teflon and glass homogenizer. The membrane suspension (25 ml aliquots in 50 ml tubes) were flash frozen in liquid nitrogen and stored at -80°C until use.

Purification: Thawed membrane suspensions (50 ml) were placed in a glass beaker in an ice bath with stirring. DDM powder (1 gram) was added to 50 ml of membrane suspension (2% DDM, final concentration), and stirring was continued on ice for 30 minutes. The sample was then filtered thru 5 µm and 2 µm filters to remove insoluble material. To the combined supernatants (50 ml), 2.7 ml of 4 M NaCl (200 mM, final concentration) and 0.9 ml of 300 mM imidazole (5 mM, final concentration) was added, and the pH was adjusted to pH 7.6 by addition of 0.5 M Na_2HPO_4 (pH 10). The extract was then loaded onto a Talon column (1.5 x 5 cm) that had been equilibrated with 50 mM NaP_i/0.01% DDM/200 mM NaCl/5 mM imidazole (pH 7.6) (Column Buffer). Non-absorbed material was washed from the column with Column Buffer, followed by washing with 50 mM NaP_i/0.01% DDM/200 mM NaCl/10 mM imidazole (pH 7.6) (Wash Buffer 2) and 50 mM NaP_i/0.2% NG (pH 7.6) **(**Wash Buffer 3) to background UV absorption. Purified protein was eluted from the column with 20mM Hepes (pH 6.5)/0.2% NG/200 mM imidazole). The protein was finally concentrated with Amicon Ultra centrifugal filters (50K MWCO) at 3500 rpm in a swinging bucket rotor to 0.2 – 0.5 ml and diluted in 15 ml of 20 mM Hepes /0.2% NG (pH 6.5) and concentrated again to ~10 mg/ml.

Table 1. Data collection and refinement statistics

Space group (no.)	$C222_1$ (20)
Cell dimensions, *a,b,c*	101.6, 121.9, 264.0
Wavelength (Å)	1.115
Resolution range (Å)	44-3.5 (3.65-3.5)[a]
No. unique reflns.	20954 (2442)
Completeness	99.4 (99.3)
Redundancy	4.1 (4.2)
I/sig(I)	6.47 (0.55)
CC(1/2)[b] in highest resln. bin	14.4
R_{meas}[c] (%)	11.2 (277.8)

Refinement

Resolution range (Å)	44-3.5 (3.65-3.5)
Completeness (%)	99.4 (99.3)
No. reflections (work/free)	20954/1077
R_{work} (%)	26.7 (44.0)
R_{free} (%)	28.7 (48.0)
No. protein atoms	6211
No. ligand atoms (TDG)	46
Wilson B-factor ($Å^2$)	167
Average B-factor, Protein ($Å^2$)	156
Average B-factor, TDG ($Å^2$)	137
r.m.s. deviations	
Bond lengths (Å)	0.005
Bond angles (Å)	0.98
Ramachandran plot	
Favored (%)	92.8
Outliers (%)	0

[a]Values in parentheses refer to the highest resolution shell.
[b]Percentage of correlation between intensities from random half-datasets
[c]Redundancy-independent R-factor (on intensities).

Table 2. Distance matrix between the residues in the partially occluded state structure and WT structure (cytoplasmic side)

Occ($) Inward(*) displac(#)	TM2 (67)	TM3 (75)	TM4 (133)	TM5 (139)	TM6 (186)	TM7 (221)	TM8 (285)	TM9 (290)	TM10 (337)	TM11 (346)	TM12 (399)
TM1 (10)	22.22($) 23.55(*) (1.33) (#)	20.79 20.00 (-0.79)	12.21 10.62 (-2.21)	12.33 11.71 (-0.61)	11.17 13.75 (2.58)	37.72 42.26 (4.54)	29.82 35.39 (5.57)	25.83 39.04 (13.21)	24.93 33.97 (9.04)	23.24 31.65 (8.41)	39.50 46.25 (8.13)
TM2 (67)	-	9.4 9.04 (-0.36)	15.16 15.98 (0.82)	19.46 18.92 (-0.54)	20.20 20.95 (0.75)	21.66 30.38 (8.72)	28.55 36.66 (8.11)	26.90 35.26 (8.36)	15.02 24.86 (9.84)	9.28 18.55 (9.27)	27.74 36.34 (8.6)
TM3 (75)		-	18.52 16.17 (-2.53)	23.26 20.19 (-3.07)	14.34 12.96 (-1.38)	31.08 38.69 (7.61)	35.08 42.32 (7.24)	34.84 41.84 (7.00)	23.64 32.56 (8.92)	18.05 29.90 (8.85)	36.94 44.01 (7.07)
TM4 (133)			-	5.63 4.34 (-1.29)	17.01 17.24 (0.23)	24.79 34.22 (9.43)	17.89 30.31 (12.42)	21.37 33.36 (11.99)	12.55 22.40 (9.85)	14.06 22.40 (8.34)	28.16 39.45 (11.29)
TM5 (139)				-	20.34 20.99 (0.65)	25.39 32.60 (7.21)	14.00 26.54 (12.54)	18.35 30.46 (12.11)	14.72 23.94 (9.22)	15.38 21.55 (6.17)	28.08 37.54 (9.46)
TM6 (186)					-	39.03 47.89 (8.86)	34.25 46.20 (11.95)	37.30 47.84 (10.54)	29.02 40.50 (11.48)	25.08 36.12 (11.04)	43.33 52.48 (9.15)
TM7 (221)						-	22.18 21.23 (-0.95)	15.66 13.80 (-1.86)	10.87 8.84 (-2.03)	14.08 12.99 (-1.09)	8.24 8.55 (0.31)
TM8 (285)							-	10.04 10.49 (0.45)	15.78 16.20 (0.42)	20.52 22.37 (1.85)	19.64 21.91 (2.27)
TM9 (290)								-	12.62 12.26 (-0.36)	18.58 19.58 (1.00)	11.77 11.95 (0.15)
TM10(337)									-	6.05 7.42 (1.37)	14.72 14.68 (-0.04)
TM11(346)										-	19.74 20.27 (0.53)

TM= Transmembrane Helix, in Parenthesis = residue number used for distance calculation. Domain 1, Residues 1-190 (N terminal); Domain 2, residues 207-410 (C terminal). In displacement, negative numbers denote the related helix goes further apart compared to inward-open structure Positive numbers denotes related helix comes closer compared to inward-open structure Occ($): Partially Occluded state distance Inward(*): Inward-open state distance displac(#):Displacement = inward open distance – occluded state distance

Yellow represents intradomain (N terminal to N terminal) distances and displacement. Green represents intradomain (C terminal to C terminal) distances and displacement. Light blue represents interdomain (N terminal to C terminal) distances and displacement.

Table 3. Distance matrix between the residues in the partially occluded state structure and the WT structure (Periplasmic side)

Occ($) Inward(*) displac(#)	TM2 (42)	TM3 (98)	TM4 (104)	TM5 (160)	TM6 (167)	TM7 (250)	TM8 (255)	TM9 (308)	TM10 (312)	TM11 (370)	TM12 (380)
TM1 (36)	10.75$ (10.7)* (-0.01)#	16.09 (16.3) (+0.20)	16.20 (16.4) (+0.18)	16.56 (14.2) (-2.32)	13.99 (14.2) (+0.23)	22.25 (14.3) (-7.94)	14.32 (11.6) (-2.69)	31.90 (23.5) (-8.33)	22.25 (18.5) (-3.72)	21.88 (15.8) (-6.07)	29.52 (21.1) (-8.43)
TM2 (42)	-	17.64 (17.34) (-0.30)	13.30 (12.26) (-1.04)	25.56 (22.7) (-2.88)	23.00 (22.62) (-0.38)	21.73 (17.0) (-4.66)	18.89 (20.4) +(1.55)	28.31 (20.08) (-8.23)	25.98 (20.7) (-5.25)	12.91 (5.36) (-7.55)	22.82 (13.79) (-9.03)
TM3 (98)		-	6.92 (8.06) (1.14)	27.21 (25.1) (-2.11)	17.16 (16.26) (-0.90)	36.49 (30.0) (-6.46)	30.14 (26.2) (-3.94)	43.3 (36.66) (-6.64)	39.45 (33.9) (-5.54)	28.1 (20.29) (-7.82)	38.3 (31.11) (-7.19)
TM4 (104)			-	29.7 (27.57) (-2.13)	21.60 (21.68) (+0.08)	33.98 (28.1) (-5.87)	29.39 (27.5) (-1.88)	39.75 (32.19) (-7.56)	37.48 (31.9) (-5.57)	22.65 (13.8) (-8.82)	34.10 (25.24) (-8.86)
TM5 (160)				-	11.97 (12.03) (+0.06)	34.1 (16.93) (-17.19)	15.66 (7.23) (-8.43)	33.64 (27.76) (-5.88)	24.03 (18.3) (-5.71)	32.31 (26.3) (-5.97)	36.02 (29.71) (-6.31)
TM6 (167)					-	31.2 (25.05) (-6.18)	22.56 (15.9) (-6.66)	40.07 (35.33) (-4.74)	32.50 (27.9) (-4.59)	32.47 (26.7) (-5.75)	39.71 (34.06) (-5.65)
TM7 (250)						-	11.1 (11.49) (+0.37)	12.66 (12.55) (-0.11)	5.37 (4.77) (-0.6)	19.55 (19.7) (+0.18)	15.86 (16.20) (+0.34)
TM8 (255)							-	23.35 (23.66) (+0.31)	13.6 (13.76) (+0.11)	23.4 (24.57) (+1.12)	24.83 (25.88) (+1.05)
TM9 (308)								-	11.85 (11.4) (-0.43)	19.8 (19.48) (-0.35)	10.06 (9.74) (-0.32)
TM10 (312)									-	23.14 (22.6) (-0.52)	18.17 (17.74) (-0.43)
TM11 (370)										-	11.89 (11.97) (+0.08)

TM= Transmembrane Helix, in Parenthesis = residue number used for distance calculation. Domain 1, Residues 1-190 (N terminal); Domain 2, residues 207-410 (C terminal). In displacement, negative numbers denote the related helix goes further apart compared to inward-open structure Positive numbers denotes related helix comes closer compared to inward-open structure Occ($): Partially Occluded state distance Inward(*): Inward-open state distance displac(#):Displacement = inward open distance – occluded state distance

Yellow represents intradomain (N terminal to N terminal) distances and displacement. Green represents intradomain (C terminal to C terminal) distances and displacement. Light blue represents interdomain (N terminal to C terminal) distances and displacement.

Table 4: Hydrogen bond distances between side chains and TDG in 2 different binding sites in the asymmetric unit (calculated in Coot)

Numbers bold and in parentheses indicate bond distances above the range of reasonable hydrogen bonds.

Protein Side chain atom	TDG atom	Distance in Chain A (A˚)	Distance in Chain B (A˚)
E269 OE1	TDG O4	2.7	3.4
E269 OE2	TDG O4	3.1	3.4
E269 OE2	TDG O3	3.0	**(4.4)**
R144 NH1	TDG O6	2.4	2.7
R144 NH2	TDG O2'	2.6	2.7
R144 NH2	E126 OE2	2.6	2.7
R144 NH2	TDG O5	**(4.0)**	3.2
R144 NH1	TDG O5	3.1	3.3
R144 NE	E126 OE2	**(3.5)**	2.8
E126 OE2	TDG O2'	2.6	2.5
E126 OE1	Y350 OH	2.5	3.2
E126 OE1	TDG O2'	2.5	2.8
H322 NE2	TDG O3	**(3.8)**	3.1
H322 ND1	Y236 OH	2.9	2.6
H322 ND1	E325 OE2	3.2	3.0
N272 ND2	TDG O4	3.4	3.4

A

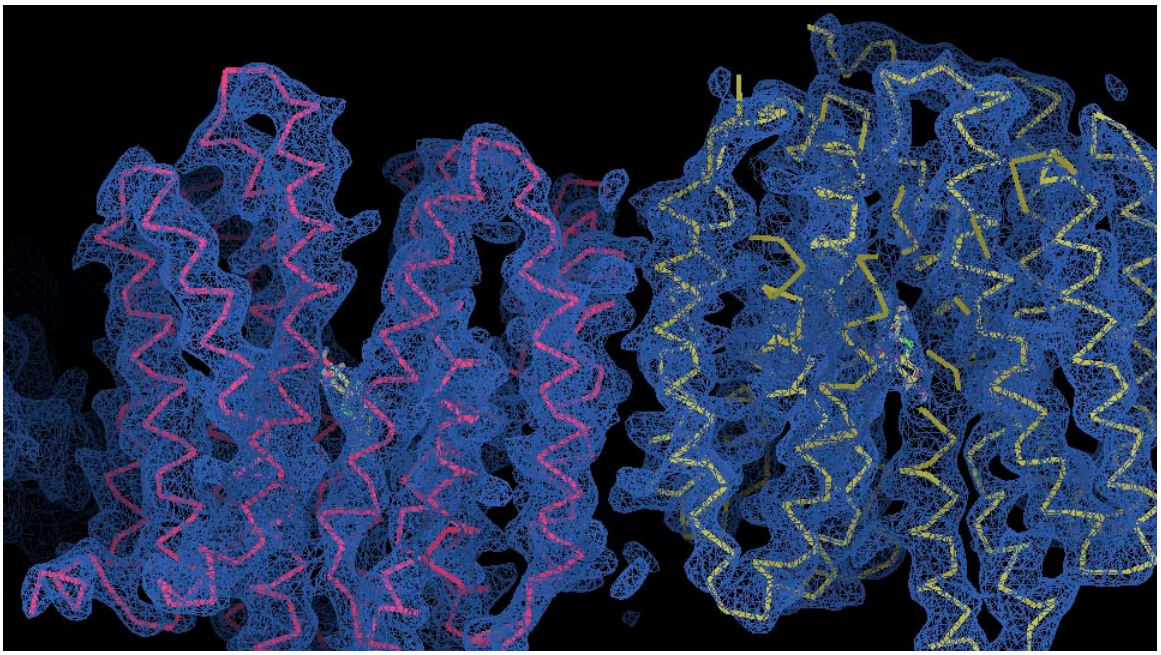

B

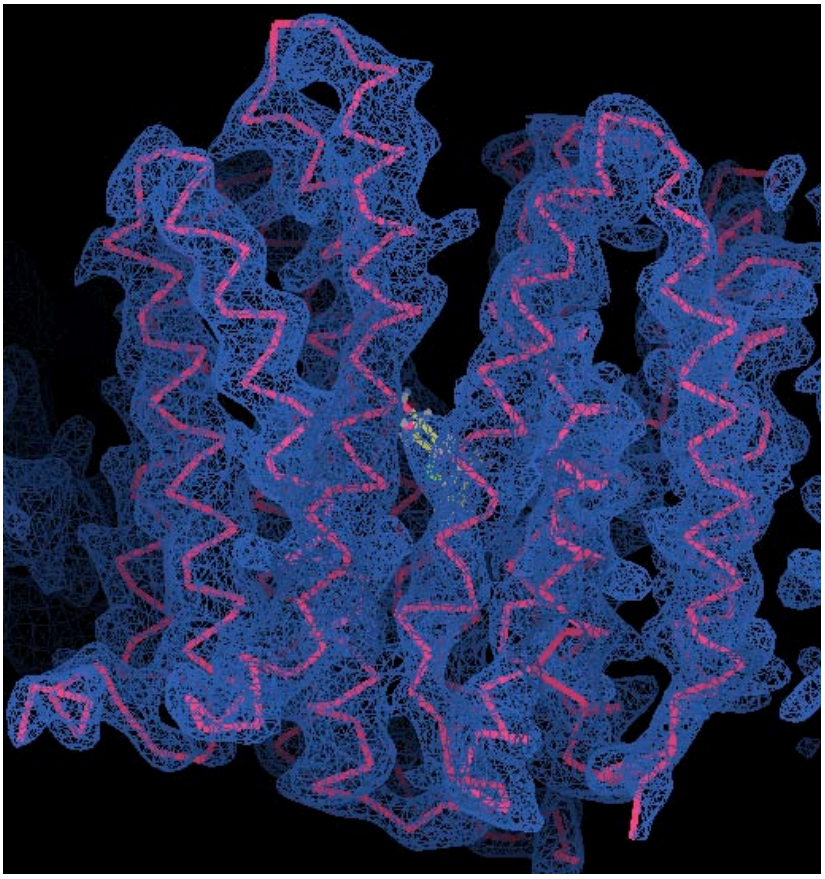

***SI Fig* 1.** LacY G46WG262W showing electron density (2mFo-DFc) map contoured at 1.5σ. No B-factor sharpening was applied.

(A) Showing the asymmetric unit

(B) Showing molecule on left in A for clarity. Periplasmic side at the top.

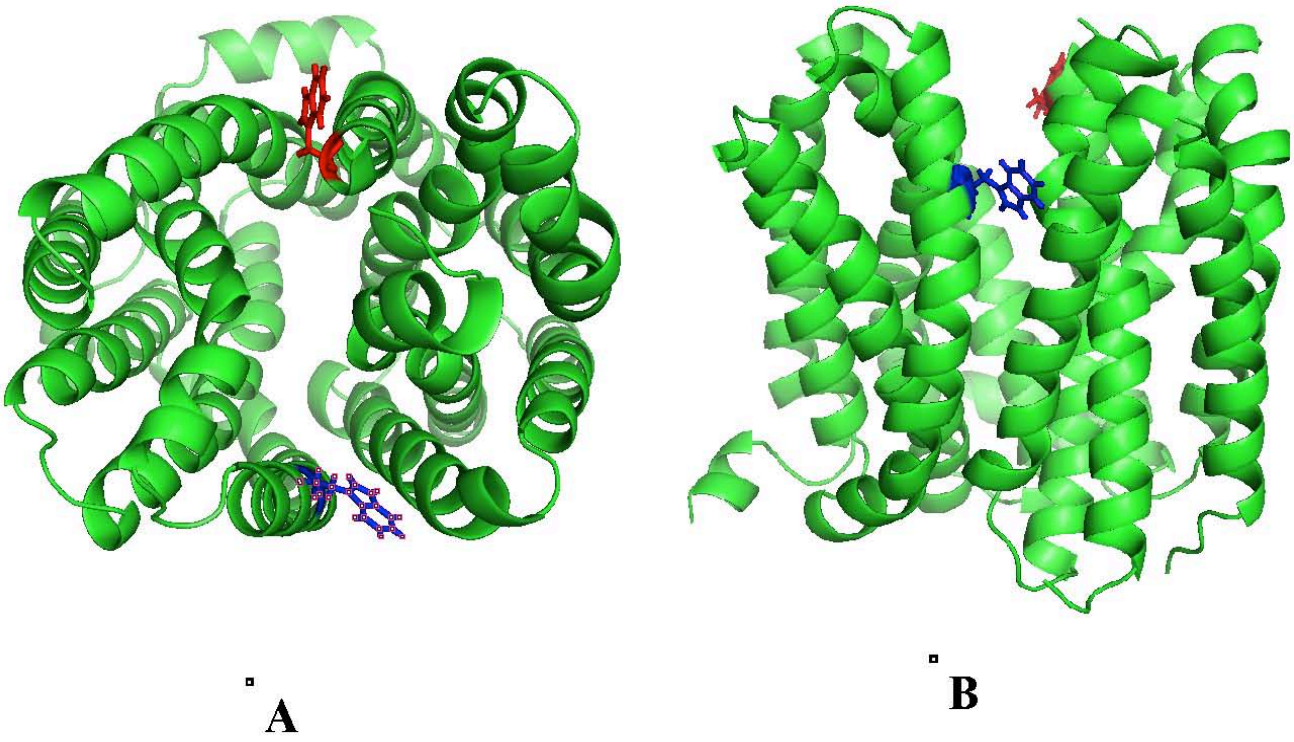

***SI Fig.* 2.** LacY G46WG262W. Partially occluded state facing outward. Showing Trp replacement at position 46 in red, and Trp replacement at positions 242 is in blue. **(A)** Periplasmic View; **(B)** Side view.

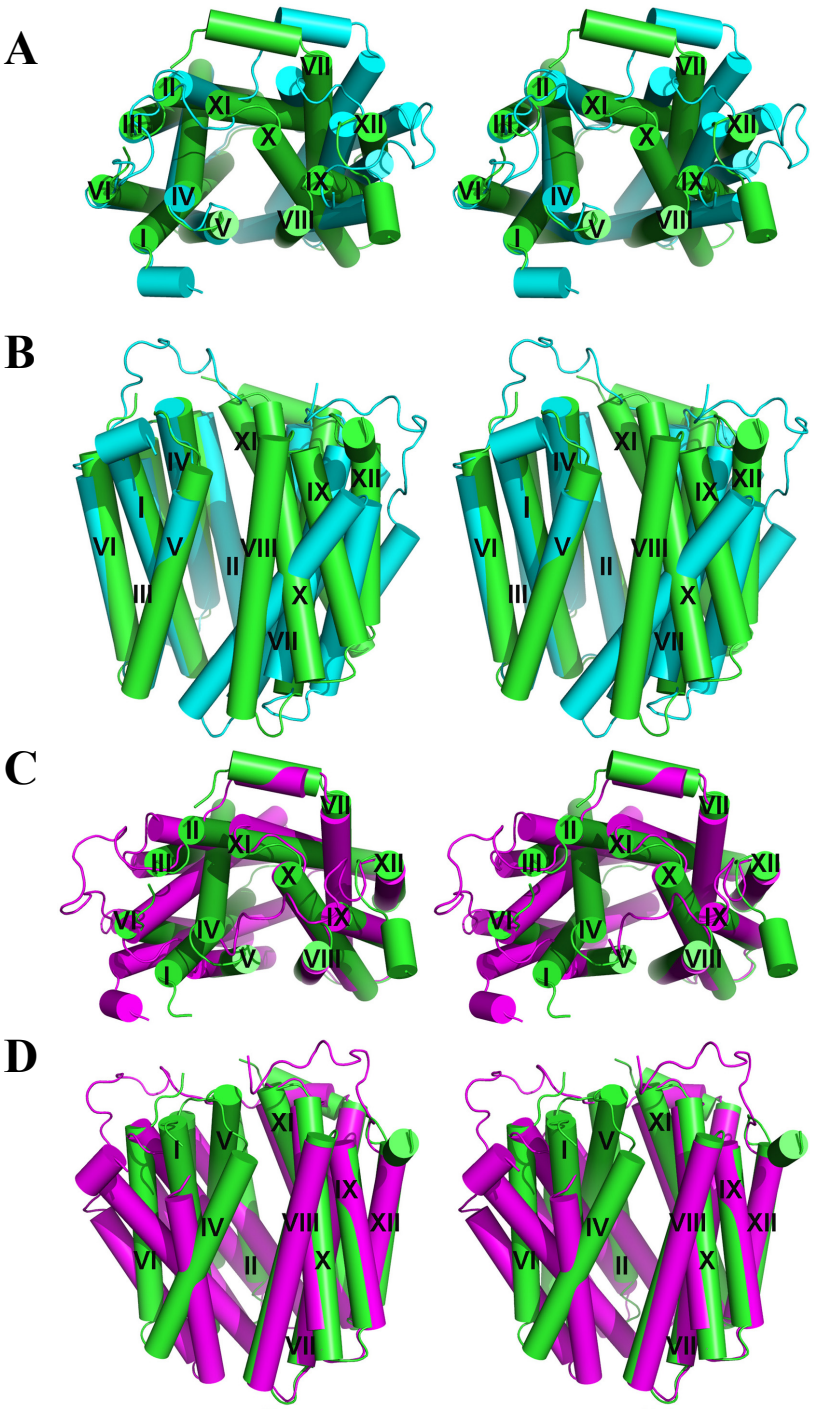

***SI Fig.* 3.** Crossed-eyes stereoscopic illustration of the conformation change between wild-type LacY and LacY G46WG262W
(A) Alignment of WT LacY (Inward Open state, blue) and LacY G46WG262W (green). Transmembrane helices are numbered in order from N-to C-terminal, and the alignment is based on helices 1-6 to emphasize the movement of the C-terminal 6 helical domain. The view is from the cytoplasmic side. **(B)** Side view from within the membrane plane with cytoplasmic surface upward. **(C)** As in A, but structural alignment based on overlap of helices 7-12 to emphasize the movement of the N-terminal domain. **(D)** as in C but viewed from the side as in B.

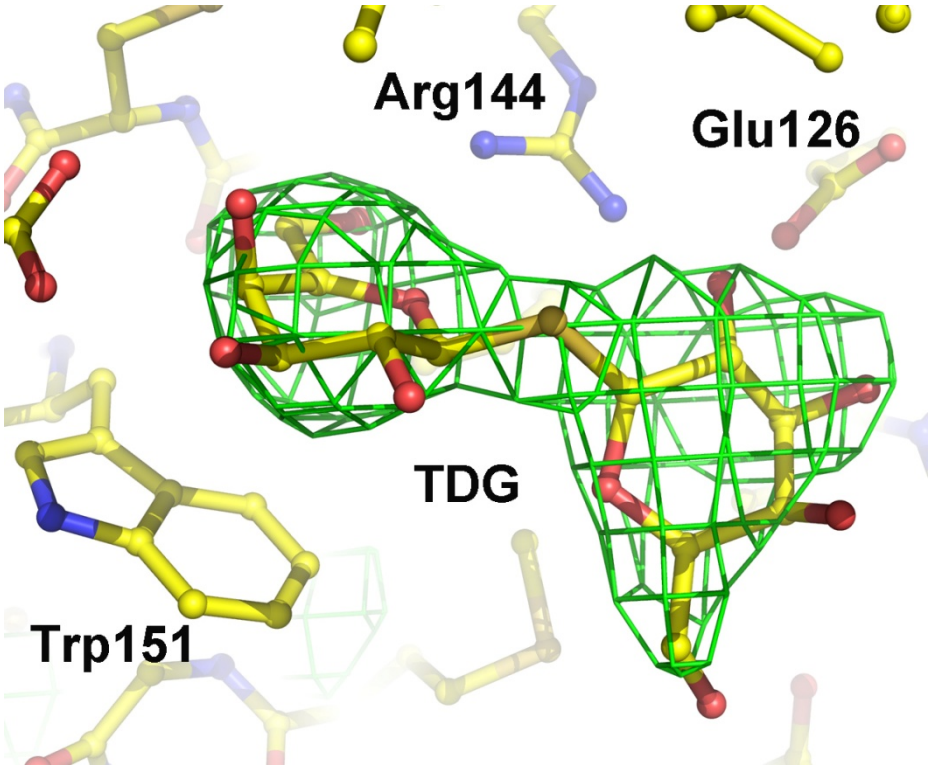

***SI Fig.* 4.** An unbiased difference electron density (mFo-DFc) map contoured at 3σ around bound TDG. The structure was solved using the apo-LacY structure (PDB ID 2CFQ), which does not have bound substrate. After further refinement without substrate, the density shown here overlaid with the ligand TDG appeared in the difference map. No B-factor sharpening was applied.